HHS Public Access

Author manuscript

Clin Cancer Res. Author manuscript; available in PMC 2024 July 05.

Published in final edited form as:

Clin Cancer Res. 2024 January 05; 30(1): 106–115. doi:10.1158/1078-0432.CCR-23-1180.

Tumor Volume Growth Rates and Doubling Times during Active Surveillance of IDH-mutant Low-Grade Glioma

Ankush Bhatia[1,2,*], **Raquel Moreno**[3,*], **Anne S Reiner**[4], **Subhiksha Nandakumar**[4], **Henry S Walch**[4], **Teena M Thomas**[3], **Philip J Nicklin**[3], **Ye Choi**[3], **Anna Skakodub**[1], **Rachna Malani**[1], **Vivek Prabhakaran**[5], **Pallavi Tiwari**[5], **Maria Diaz**[1], **Katherine S. Panageas**[4], **Ingo K Mellinghoff**[1], **Tejus A Bale**[6,^], **Robert J Young**[3,^]

[1]Department of Neurology, Memorial Sloan Kettering Cancer Center, New York City, New York.

[2]Department of Neurology, University of Wisconsin School of Medicine and Public Health, Madison, WI.

[3]Department of Radiology, Memorial Sloan Kettering Cancer Center, New York City, New York.

[4]Department of Epidemiology and Biostatistics, Memorial Sloan Kettering Cancer Center, New York City, New York.

[5]Department of Radiology, University of Wisconsin School of Medicine and Public Health, Madison, WI.

[6]Department of Pathology and Laboratory Medicine, Memorial Sloan Kettering Cancer Center, New York City, New York.

Abstract

Purpose: Isocitrate-dehydrogenase-mutant (IDH-mt) gliomas are incurable primary brain tumors characterized by a slow-growing phase over several years followed by a rapid-growing malignant phase. We hypothesized that tumor volume growth rate (TVGR) on magnetic resonance imaging may act as an earlier measure of clinical benefit during the active surveillance period.

Experimental Design: We integrated 3-dimensional volumetric measurements with clinical, radiological, and molecular data in a retrospective cohort of IDH-mt gliomas that were observed after surgical resection in order to understand tumor growth kinetics and the impact of molecular genetics.

Corresponding author: Ankush Bhatia, MD, 7275 UW Medical Foundation, Centennial Building (MFCB), 1685 Highland Avenue, Madison, WI 53705. Phone: 608-263-5448; bhatia@neurology.wisc.edu.

*Ankush Bhatia and Raquel Moreno contributed equally as co-first authors.

^Tejus A Bale and Robert J Young contributed equally as co-senior authors.

Conflict of interest disclosure statement:

Ankush Bhatia, Raquel Moreno, Anne S Reiner, Subhiksha Nandakumar, Henry S Walch, Teena M Thomas, Philip J Nicklin, Ye Choi, Anna Skakodua, Rachna Malani, Maria Diaz, Vivek Prabhakaran, Pallavi Tiwari, and Tejus Bale have no COI to disclose. Robert J Young has consulted for ICON plc, NordicNeuroLab, Olea Sphere, and owns stock in Agios. Katherine S. Panageas receives funding from AACR Project GENIE. Ingo K Mellinghoff reports serving as a consultant for 501c3 Global Coalition for Adaptive Research; reports honoraria from the Doris Duke Charitable Foundation; reports serving on advisory board for Black Diamond Therapeutics, Roche Therapeutics, Prelude Therapeutics Incorporated, Voyager Therapeutics; reports research support from Erasca Therapeutics, Servier Pharmaceuticals LLC, Kazia Therapeutics, Vigeo Therapeutics, and Samus Therapeutics, Inc

Results: Using log-linear mixed modeling, the entire cohort (n=128) had a continuous %TVGR per 6 months of 10.46% (95% CI: [9.11%, 11.83%]) and a doubling time of 3.5 years (95% CI: [3.10-3.98]). High molecular grade IDH-mt gliomas, defined by the presence of homozygous deletion of CDKN2A/B, had %TVGR per 6 months of 19.17% (95% CI: [15.57%, 22.89%]) which was significantly different from low molecular grade IDH-mt gliomas with a growth rate per 6 months of 9.54% (95% CI: [7.32%, 11.80%]) ($P < 0.0001$). Using joint modeling to co-model the longitudinal course of TVGR and overall survival, we found each one natural logarithm tumor volume increase resulted in more than a 3-fold increase in risk of death (HR=3.83, 95% CI: [2.32-6.30], $P < 0.0001$).

Conclusions: TVGR may be used as an earlier measure of clinical benefit and correlates well with the WHO 2021 molecular classification of gliomas and survival. Incorporation of TVGR as a surrogate endpoint into future prospective studies of IDH-mt gliomas may accelerate drug development.

Keywords

neuro-oncology; genomics; glioma; tumor volume; surrogate endpoint

Introduction

Isocitrate dehydrogenase-mutant low-grade gliomas (IDH-mt LGGs) are rare, eventually fatal malignant brain tumors found primarily in young adults (1-3). After maximal safe resection, IDH-mt LGGs are often characterized by a slow-growing phase lasting several years, followed by a rapid-growing, malignant phase (1,2,4). Optimal timing to initiate radiation and chemotherapy for resected IDH-mt LGGs during the slow-growing phase is controversial amongst oncologists (4,5) due to significant treatment-related morbidity associated with chemoradiation (6), and has resulted in some oncologists favoring a “watch and wait” strategy (7,8). This period of watchful waiting, or active surveillance, is a prime opportunity to introduce less morbid, novel, targeted therapies that might prolong the time before chemoradiation; however, this will require development of surrogate endpoints for monitoring of disease progression.

Radiographic endpoints have historically relied on 2-dimensional (2D) measurements on magnetic resonance imaging (MRI), but 2D measurements do not reliably reflect the biology during the slow-growing phase. Furthermore, reliance on traditional endpoints such as overall or progression-free survival in clinical trials are not realistic since previous studies have taken several years to determine a clinical benefit (9-12). 2D measurements of tumor size carry significant limitations due to subtle signal changes on T2/fluid attenuated inversion recovery (FLAIR) images, irregular shapes and growth in different directions, residual glial scarring, heterogeneous acquisition tilt, and Wallerian degeneration (9). Previous studies that have focused on 2D measurements or volume of diametric expansion (VDE) report that untreated LGGs grow at a rate of about 3-5 mm in tumor diameter per year (13,14). While these important data have also correlated with overall survival in large retrospective studies (15-17), limitations in 2D measurements have hampered implementation into clinical practice.

More recently, investigators explored volumetric (3D) analysis of IDH-mt LGGs as a novel surrogate endpoint to overcome barriers of 2D measurements. One retrospective study on a limited number of scans at various time points during the untreated disease course demonstrated differences in tumor volume growth rate (TVGR) between 1p19q codeleted and 1p19q intact gliomas (18). Additionally, a recent study demonstrated 3D measurements were superior compared to 2D measurements in non-enhancing IDH-mutant LGGs with higher inter-reader agreement and lower growth rate variability with 3D measures (19). However, while volumetric analyses are encouraging, foundational work that links comprehensive molecular profiling, with tumor growth rates, clinical variables, and radiological characteristics are needed.

As novel IDH-targeted therapies are evaluated in clinical trials (20-23), there is a need to refine current radiographic evaluation of IDH-mt LGGs to more accurately predict tumor growth trajectories and capture the biology of IDH-mt LGG (24). As a first step in developing surrogate endpoints of disease progression during the watch and wait active surveillance period, we analyzed a large cohort of patients with resected IDH-mt LGGs that received no upfront chemoradiation; an important group that (1) is historically considered “low-risk”, (2) has no natural history data, and (3) is the target population of future therapeutic clinical trials. We integrated 3D volumetric segmentation with clinical, radiological, and molecular data to establish the relationship between tumor size and tumor growth kinetics with molecular genetics.

Methods

Patient Selection

This retrospective study was granted a waiver of informed consent by the local institutional review board and was performed in compliance with Health Insurance Portability and Accountability Act regulations as well as the Declaration of Helsinki. We identified 128 consecutive adult patients with WHO 2016 Grade 2 IDH-mutant astrocytoma or oligodendroglioma evaluated at Memorial Sloan Kettering Cancer Center (MSKCC) between 1997 and 2019 that met our inclusion/exclusion criteria (Figure 1). Inclusion criteria were (1) age ≥ 18 years, (2) histopathologic diagnosis of IDH-mutant WHO Grade 2 glioma, (3) MRI of the brain with and without contrast performed at least twice six months apart after diagnostic biopsy or resection, and (4) underwent active surveillance after diagnostic biopsy or resection. Patients were excluded if (1) they received postoperative treatment with radiation and/or chemotherapy, (2) they had higher grade histology (Grade 3 or 4), (3) they had any amount of enhancement on postoperative post-contrast T1 imaging made at least one month from surgery to minimize measuring post-operative changes and/or conversion to higher grade tumor, or (4) MRI artifact precluded imaging analysis. Clinical data included age at diagnosis, sex, presenting neurological symptoms (seizure, headache, cognitive dysfunction, motor or sensory symptoms, dizziness, word finding difficulty), and dates of surgery, radiation, and chemotherapy (summarized in Table 1). Study data were collected and managed using Research Electronic Data Capture (REDCap) tools hosted at MSKCC (25,26).

MRI Acquisition

MRI was performed on 1.5T or 3T systems (mostly 750w/450w, GE Healthcare, Milwaukee, WI). As most of the study period predated the consensus brain tumor imaging protocol recommendations,(10) conventional MRI was acquired using variable parameters but including pre- and post-contrast images (including either 2D or 3D T2-weighted [T2w] and/or T2w fluid attenuated inversion recovery [FLAIR] images, as well as contrast-enhanced T1-weighted images). MRI slice thickness was no more than 5 mm with an interslice gap of no more than 1.5 mm.

Image Segmentation, Volumetrics, and Feature Description

All qualified MRI studies performed during the period of active surveillance underwent manual volumetric segmentation of the T2/FLAIR abnormality using iNtuition 4.4.13 (Tera Recon) performed by a trained operator and/or neuroradiologist (R.M., with > 5 years of experience) followed by a secondary review and verification by an experienced neuroradiologist (R.J.Y, with > 20 years of experience). A modified VASARI (Visually AcceSAble Rembrandt Images) MRI feature set was also used to describe features on the preoperative imaging when available. Features included the T2-FLAIR mismatch sign (T2 bright, FLAIR dark), which has been described as having high specificity for identifying IDH mutant 1p19q intact astrocytomas due to the microcystic changes in protoplastic astrocytomas (27-29). Feature assignment was performed by a board-certified neuroradiologist (R.M.) and verified by an experienced neuroradiologist (R.J.Y.). Image segmentation was performed sequentially on all MRIs available during the period of active surveillance. The segmented contour was drawn to exclude nontumor regions such as hemorrhage, surgical cavity, or postoperative changes as determined with the help of the other sequences. The T2/FLAIR volume (in cubic centimeters) was calculated by multiplying the total pixel counts with pixel volume. Volumes were then automatically extracted from TeraRecon and transferred into REDCap using a custom-built in-house application programming interface (API). To further investigate the impact of growth rates on molecular genetics, patients were stratified into slow growth, intermediate growth, and fast growth, which were defined by the bottom quartile, middle 50%, and top quartile, respectively, using the distribution of the individually-modeled growth rates, further described below in the statistical analysis section.

Neuropathologic and Molecular Analysis

Tumor material obtained from neurosurgical initial biopsy or resection was reviewed by an experienced molecular neuropathologist (T.B.) and an integrated diagnosis, in keeping with WHO 2016/2021 molecular classification criteria (30), was rendered as follows: All patients were verified to be IDH-mutant by immunohistochemistry and/or next-generation sequencing. When tissue from initial diagnostic surgery was available for further sequencing, genomic DNA was extracted from formalin-fixed paraffin-embedded samples and mutational analysis performed using Memorial Sloan Kettering-Integrated Mutation Profiling of Actionable Cancer Targets (MSK-IMPACT), a targeted hybrid capture next-generation sequencing-based DNA sequencing panel of 468 cancer genes with a corresponding matched or pooled normal sample. Samples with pooled normals

were manually reviewed to ensure the accuracy of the variants that were called and to exclude potential germline variants. MSK-IMPACT covers protein-coding exons of cancer-associated genes, as described previously (31,32) and detect somatic single nucleotide variants, insertions, deletions, copy number alterations, and certain gene fusions and structural variants. To further analyze the impact of molecular sequencing beyond IDH and 1p19q status on TVGRs, each molecular profile was reviewed by a molecular neuropathologist (T.B.) and classified as “molecular grade- low, intermediate, or high.” “Molecular grade-high” was defined by detection of homozygous deletion of CDKN2A/2B, which denotes WHO grade 4 tumors in the 2021 WHO classification of CNS Tumors (33). “Molecular grade-intermediate” was defined by alterations previously suggested to be associated with aggressive behavior in some studies, but not yet included among established grading criteria under current guidelines. “Molecular grade-intermediate” molecular profiles in 1p19q intact tumors were those (1) containing focal amplification of genes including *MYCN*, cyclic dependent kinase (CDK) genes (including CDK4) or receptor tyrosine kinase (RTK) including genes (including PDGFRA), (2) high levels of copy number variations (CNV) defined by > 3 broad chromosomal gains/losses. “Molecular grade-intermediate” molecular profiles in 1p19q codeleted tumors were those (1) mutations in the *PIK3R1* and *PIK3CA*, (2) > 3 broad chromosomal gains/losses (in addition to 1p19q loss), or (3) TP53 mutations. “Molecular grade-low” profiles were defined by the absence of “high” and “intermediate” grade molecular features, as described above (34-39).

Outcomes

Next intervention-free survival (NIFS) was defined as the date of the initial diagnostic biopsy or resection to the first date of re-resection, initiation of radiation or chemotherapy, or death for those with an event or, for those who were censored, until last follow-up. Overall survival (OS) was defined as the date of the initial diagnostic biopsy or resection to the date of death for those who had an event or until the date of last follow-up for those who were censored.

Statistical Analysis

Descriptive statistics such as proportions, medians, and interquartile ranges (IQR), were used to characterize the cohort. Demographics and clinical characteristics were compared across 1p19q status and separately across simple/complex status using Chi-squared and Fisher’s exact tests as appropriate for categorical variables and the Wilcoxon two-sample test for continuous variables. Tumor volume growth was modeled using a 1) linear and a 2) log-linear mixed-effects model weighted by follow up time per patient. The adjusted r^2 value was compared between models and the log-linear mixed-effects model was chosen for subsequent data analysis. Thus, TVGR was modeled as a constant exponential growth rate per six-month periods. To describe the distribution of growth rates, individual patient trajectories were modeled. To characterize the growth rate of the cohort in general, all patient trajectories were modeled together and weighted by the maximum follow-up time per patient. Interaction terms were modeled to compare TVGR across categories of interest. In order to evaluate the association between longitudinal MRI volume and survival (NIFS and OS separately) data, a joint model was fit. All statistical tests were two-sided with an alpha

level of statistical significance < 0.05. All analyses were performed using SAS version 9.4 (Statistical Analysis System, RRID:SCR_008567).

Data Availability

The data generated in this study are available for download in Synapse (https://www.synapse.org/#!Synapse:syn52658621/files/) and for visualization in cBioPortal (https://cbioportal.org/study/summary?id=difg_msk_2023).

Results

Clinical Characteristics

A total of 128 IDH-mutant Grade 2 (based on WHO 2016 criteria) glioma patients were included in the study, with 69 (53.9%) 1p19q codeleted and 59 (46.1%) 1p19q intact patients (Figure 1, Table 1). There were no significant differences in sex, presenting neurological symptoms, number of MRI scans, or follow up by 1p19q status. During the postoperative period after diagnostic surgery or the active surveillance period, there was a statistically significant difference in age by 1p19q status; 1p19q codeleted patients were significantly older with a median age at diagnosis of 41.3 years (IQR, 35.2 – 50.4) vs 1p19q intact patients at 32.8 years (IQR, 26.2 – 39.3). The most common presenting neurological symptoms were seizures in 80 (62.5%) patients, headaches in 19 (14.8%) patients, and cognitive changes in 11 (8.6%) patients. IDH status was verified for the entire cohort (n = 128) by IDH immunohistochemistry (n = 120 or 93.8%) and/or next-generation sequencing (n = 73 or 57%). The median number of MRI scans available for analysis during the postoperative period after diagnostic surgery was 8 (range, 2-28) for the entire cohort. The median follow up was 6.3 years (range, 0.5-23.1) in all patients.

Modeling Tumor Volume Growth

After plotting tumor volume growth on MRI per patient over time in the postoperative phase, we observed that some tumor growth appeared linear whereas some tumor growth appeared exponential (Figure 2A). We fit two separate models where the growth for each patient was individualized either linearly or exponentially (log-linear). Consistent with prior literature, the adjusted r^2 value for the mixed effects exponential model was slightly better at a value of 0.9864 compared to that of the linear model which also fit the data well but at a lower value of 0.9556. We proceeded to use the log-linear mixed effects modelling framework for tumor volume growth in subsequent analyses, presenting TVGRs per 6-month intervals.

TVGR Change during Active Surveillance

Using log-linear mixed modeling, the entire cohort (n = 128) had an overall % TVGR per 6 months of 10.46% (95% CI: [9.11%, 11.83%]) during the postoperative period after diagnostic surgery prior to any chemotherapy and radiation (Table 2). The 25^{th} percentile TVGR % per 6 months was 6.73% (95% CI: [4.54%, 7.89%]), 50^{th} percentile TVGR per 6 months was 10.62% (95% CI: [9.61%, 13.43%]), and 75^{th} percentile TVGR per 6 months was 19.92% (95% CI: [15.22%, 22.89%]) (Figure 2B). When evaluating 1p19q status, there were no significant differences in % TVGR per 6 months in the postoperative phase with

1p19q intact tumors growing at 11.73% (95% CI: [9.11%, 14.41%]) compared with 1p19q codeleted tumors growing at 9.62% (95% CI: [8.26%, 10.99%]) ($P = 0.16$) (Table 2).

Initial Tumor Size and Extent of Resection with TVGR during Active Surveillance

In the postoperative active surveillance phase, extent of resection was defined into groups based on remaining residual disease. There were no significant differences between postoperative tumor size with smaller tumors <25 cm^3 growing at 10.55% (95% CI: [8.94, 12.19%]) vs larger tumors with ≥25 cm^3 residual disease growing at 10.06% (95% CI: [8.37%, 11.78%] ($P = 0.68$). Further evaluation using recently published consensus data defining extent of resection as near total resection (0.1 cm^3 to 5 cm^3), subtotal resection (>5 cm^3 to <25.0 cm^3), or partial resection (≥25 cm^3)(40) did not demonstrate any significant differences in TVGR between any subgroups based on 1p19q status or extent of resection ($P \geq 0.20$) (Table 2).

Doubling Time During Active Surveillance

The doubling time during the postoperative phase, calculated in 12-month or yearly periods, was 3.5 years (95% CI: [3.10-3.98]). Further delineation based on 1p19q status revealed similar doubling times (Table 3) with 1p19q codeleted tumors doubling in 3.8 years (95% CI: [3.32-4.37]) and 1p19q intact tumors doubling in 3.1 years (95% CI: [2.57-3.98]).

TVGR and Next Generation Molecular Sequencing

Seventy-three IDH-mt LGG patients underwent next-generation sequencing using MSK-IMPACT. Samples were separated into two groups based on their 1p19q status: codeleted (oligodendroglioma) and intact (astrocytoma). The genetic profiles in the entire cohort were typical for IDH-mutant gliomas, and the TVGRs varied per patient (top row) (Supplementary Figure S1). The most common genomic alterations in the 1p19q codeleted group were TERT promoter mutations (100%), CIC (42%) and FUBP1 (24%), consistent with previous studies. Conversely, in the 1p19q intact group the most frequently altered genes were TP53 (94%) and ATRX (77%).

TVGR was first examined from the perspective of molecular grading using specific criteria based on previously published literature described above in the Methods section. Forty-eight patients met criteria for molecular grade-low, 21 patients for molecular grade-intermediate, and 4 patients for molecular grade-high (Table 4). Molecular grade-high IDH-mt gliomas, characterized by the presence of CDKN2A/2B homozygous deletion, grew significantly faster at 19.17% (95% CI: [15.57%, 22.89%]) compared with molecular grade-intermediate (9.09%, 95% CI: [6.76%, 11.46%]) and molecular grade-low (9.54%, 95% CI: [7.32%, 11.80%]) (Figure 2C). Representative neuroimaging of each molecular grade is shown with patient examples in Figure 2D. Specific alterations in molecular grade-high group are shown in Supplementary Table S1. In a post-hoc analysis, low plus intermediate molecular grade groups were combined demonstrating a TVGR% of 9.37% (95% CI: [7.72%-11.05%]), still significantly different from the molecular grade high group TVGR% of 19.17% (95%CI: 15.57%-22.89%).

We then examined molecular grading from the perspective of tumor volumetrics by stratifying patients with slow, intermediate, and fast growing IDH-mt gliomas (also defined in methodology based on distribution of TVGRs). These attempts to characterize molecular genetics based on TVGRs using slow, intermediate, and fast criteria (as defined in methodology) demonstrated no significant differences (Supplementary Figure S2A, S2B). Lastly, tumor mutational burden and fraction genome alterations in the entire cohort demonstrated no differences between slow, intermediate, and fast TVGRs. (Supplementary Figure S2C).

Tumor Volume Change during active surveillance as a predictor of NIFS and OS

Using joint modeling to co-model the longitudinal course of MRI-based tumor volume growth and NIFS, we found for each one natural logarithm tumor volume increase, risk of next intervention or death increased 61% (HR = 1.61, 95% CI: [1.33-1.95], $P < 0.0001$). For each 10% increase in MRI-based tumor volume, there was a 5% increase in risk of next intervention or death (95% CI: [3%-7%]). Using similar analysis for OS, we found for each one natural logarithm tumor volume increase, risk of death increased more than 3-fold (HR=3.83, 95% CI: [2.32-6.30], $P < 0.0001$). For each 10% increase in MRI-based tumor volume, there was a 14% increase in risk of death (95% CI: [8%-19%]). Tumor volume change was statistically significantly associated with both NIFS and OS. NIFS and OS data are plotted in Supplementary Figure S3.

Preoperative Clinical and Radiological Characteristics

Preoperative MRIs were analyzed for VASARI features when available. Preoperative and postoperative tumor volumes were not significantly different between 1p19q codeleted and 1p19q intact tumors (Supplementary Table S2). The T2-FLAIR mismatch sign was present in 21 (38.9%) 1p19q intact patients and absent in 63 (96.9%) of 1p19q codeleted patients ($P < 0.0001$). T2 heterogeneity was present more frequently in 1p19q codeleted tumors vs 1p19q intact tumors (53.7% vs 27.3%, respectively, $P = 0.003$). Necrotic and/or cystic features were present significantly more in 1p19q codeleted tumors than 1p19q intact tumors (29 (43.3%) patients vs 14 (24.6%) patients, respectively, $P = 0.03$). Diffusion characteristics were also significantly different by 1p19q status ($P = 0.004$) with mixed diffusion occurring in 27 (45%) 1p19q codeleted tumors compared with 9 (18%) 1p19q intact tumors. Other radiological characteristics such as side, FLAIR extension, eloquent area, enhancement, margins, hemorrhage, deep white matter, peritumoral edema, or intratumoral vessels, were not significantly different by 1p19q status.

Preoperative radiological characteristics were analyzed with respect to molecular complexity. The T2/FLAIR mismatch sign was statistically significantly more present in molecular high grade (100%) compared with molecular low (13.5%) and intermediate (14.3%) grade IDH-mt gliomas ($P = 0.008$). There were no other statistically significant differences between radiological characteristics and genetic profiles (Supplementary Table S3). Finally, preoperative clinical characteristics were examined with respect to TVGR and no significant differences were found (Supplementary Table S4).

Discussion

Treatment advances in diffuse gliomas will depend on novel surrogate endpoints of disease progression. This has become particularly evident in IDH-mt gliomas where novel therapies entering later phase clinical trials require a radiographic surrogate endpoint during the period of active surveillance. Advanced neuroimaging using 3D volumetric analysis has been proposed in recent retrospective studies; however, a fundamental understanding of TVGR is needed with regards to the behavior of gliomas during active surveillance and any potential influence from clinical or molecular factors (19,41). In this retrospective study of a large cohort of molecularly characterized IDH-mt LGGs, we integrated clinical, radiological, and genomic features with tumor volume growth kinetics. This study demonstrates that IDH-mt LGGs grew continuously at a rate of about 10% per 6-month interval. This 10% growth rate was consistently demonstrated during the observational period regardless of initial tumor size or extent of resection. However, IDH-mt, 1p19q intact gliomas with aggressive molecular alterations such as CDKN2A/2B deletions had significantly faster TVGRs. Additionally, changes in growth rates over time were associated with worse prognosis. A 10% increase in tumor volume increased the risk of death 14%. Taken together, these results are a first step in implementing TVGR as a surrogate endpoint in IDH-mt gliomas during active surveillance.

This study meticulously incorporated volumetrics from every single MRI time point performed during the untreated disease course as opposed to prior volumetric studies which selected a few representative time points from which analyses were based on (18). Therefore, we consider the calculated ~10% TVGR every 6 months in the entire cohort as an accurate reflection of growth during this pre-chemoradiation slow growing phase, as opposed to ~27% growth in 6 months reported in a previous study, possibly an overestimation of growth due to fewer and later time points analyzed as well as lack of depth in genomic evaluation. Several of the initial landmark studies led by Johan Pallud et al. focusing on the growth rate in Grade 2 IDH-mutant tumors calculated tumor volume using an ellipsoid approximation based on manual measurements in the 3 largest tumor diameters, which was then used to calculate mean tumor diameter as the growth measure (15,16,42-44). This method is simpler and faster, but may overestimate tumor volume since gliomas grow in unpredictable non-ellipsoid shapes. Importantly though, this early work demonstrated a strong statistical relationship on individual tumor growth on survival and prognosis. However, no prior study to our knowledge has incorporated next-generation sequencing and radiological features as done in this study, which is necessary prior to integrating into clinical trials in the molecular era.

Our data examined the impact of the genomic features on growth kinetics in IDH-mt LGG. During the active surveillance period after maximal safe resection, IDH-mt gliomas that harbored CDKN2A/2B homozygous deletion grew significantly faster as %TVGR/6 months than IDH-mt gliomas without this molecular alteration. This finding aligns with recent changes to the WHO 2021 classification, which now defines IDH-mt, 1p19q intact gliomas with CDKN2A/2B deletion as Grade 4 IDH-mt gliomas. Additionally, this further supports the implementation of TVGR into future clinical trials as a surrogate endpoint that is consistent with integrated molecular grading. The fact that statistical significance was not

found during this observational phase based on 1p19q status raises the possibility that the survival benefit in 1p19q codeleted gliomas may be secondary to their chemosensitivity, and not necessarily inherent to their natural growth trajectory prior to treatment. This is the first study to our knowledge that studied molecular genetics on growth rates, and therefore, future studies with larger sample sizes and longer follow up will clarify these results.

In addition to volumetrics, we also examined multiple preoperative radiological characteristics of low-grade IDH-mutant gliomas. Our data are consistent with several recent meta-analyses and reviews that have shown the T2-FLAIR mismatch sign is highly specific but variably sensitive for predicting IDH mutant, 1p19q intact status in lower grade astrocytomas (27-29). Furthermore, the T2/FLAIR mismatch sign correlates with higher molecular-grade IDH-mt gliomas. To our knowledge, this is a novel finding that has not been reported in previous studies and should be explored further as a possible predictive biomarker of higher molecular grade.

Our study has several potential limitations. This was a retrospective, single-center study which limits broader application of its findings. Tumor volume segmentation was performed by trained operators and overseen by an expert neuroradiologist. These investigators were blinded to the clinical history, mutation status, and outcomes of each patient; however, there is the possibility that edema or post-surgical changes were segmented instead of tumor as these may be indistinguishable on MRI. Technical factors such as slice thickness, interslice gap, and MRI type could affect volume measurements. The scan parameters were relatively consistent. However, for patients scanned on older imaging protocols (i.e., when thicker slices and interslice gaps were the standard of care), the same scan parameters were retained at follow up, in order to mitigate any potential inaccuracies as we examined volumes over time. Future work including advanced MRI and PET may improve delineation of tumor volume and improvements in tumor volume measurements that can be achieved by utilizing standardized brain tumor imaging protocol guidelines (10), which were published after most of the scans in our retrospective cohort. The potential future impact of rapidly advancing artificial intelligence (AI) and other automated segmentation algorithms cannot be overlooked, however, their current emphasis has been on analyzing treatment-naïve tumors and rather than resected or partially resected tumors (45,46).

Another area for further discussion is our molecular grade stratification. We formed molecular grade groupings with high grade defined only by CDKN2A/B deletions, aligning with the recent changes to the WHO 2021 classification of gliomas. CDKN2A/B homozygous deletion in Grade 2 IDH-mutant astrocytomas is indeed rare, with some conflicting evidence as to its prognostic significance, despite the clear WHO criteria designating the tumor as Grade 4 (38,47,48). Our high molecular-grade group (n=4) is a small number and therefore may impact the precision of our results for this subgroup, yet given the rarity and statistical significance of this finding, we do feel it is clinically meaningful. Additionally, an argument could be made to include other alterations in the high molecular grade group such as PDGFRA amplifications, CDK4 amplifications, and PI3K mutations, in view of previously reported associations with poor prognosis and shorter survival among patients with IDH-mutant astrocytic gliomas (35,36,49,50). Since these alterations require additional investigation and have not yet risen to the level of

evidence for incorporation into WHO grading, we incorporated them into an intermediate molecular grade group. Importantly, we demonstrated that this intermediate molecular grade group did not grow significantly faster than the low molecular grade group. Future studies could explore the impact of alterations at the whole genome level, protein level, and/or posttranslational modifications.

The optimal management of IDH-mt LGGs remains nebulous with heterogeneous treatment practices mostly due to incomplete understanding of the natural history of disease. As novel targeted therapies enter later-stage clinical trials, there is an urgent need for surrogate endpoints to more effectively measure outcomes. Further prospective validation studies of MRI TVGRs will be helpful to determine the utility of volumetrics as a novel surrogate endpoint for drug development in IDH-mt LGGs.

Supplementary Material

Refer to Web version on PubMed Central for supplementary material.

Acknowledgements:

The authors are grateful to the MSK Radiology Informatics Team and the imaging processing technologists in the 3D Sloan Advanced Imaging Laboratory (SAIL). The authors would like to thank James P. Zacny, PhD for editorial assistance. This work was supported by Memorial Sloan Kettering Cancer Center Support Grant/Core Grant P30 CA008748.

References

1. van den Bent MJ, Smits M, Kros JM, Chang SM. Diffuse Infiltrating Oligodendroglioma and Astrocytoma. J Clin Oncol 2017;35(21):2394–401 doi 10.1200/JCO.2017.72.6737. [PubMed: 28640702]
2. Schiff D, Van den Bent M, Vogelbaum MA, Wick W, Miller CR, Taphoorn M, et al. Recent developments and future directions in adult lower-grade gliomas: Society for Neuro-Oncology (SNO) and European Association of Neuro-Oncology (EANO) consensus. Neuro Oncol 2019;21(7):837–53 doi 10.1093/neuonc/noz033. [PubMed: 30753579]
3. Yan H, Parsons DW, Jin GL, McLendon R, Rasheed BA, Yuan WS, et al. IDH1 and IDH2 Mutations in Gliomas. New Engl J Med 2009;360(8):765–73 doi DOI 10.1056/NEJMoa0808710. [PubMed: 19228619]
4. Pala A, Coburger J, Scherer M, Ahmeti H, Roder C, Gessler F, et al. To treat or not to treat? A retrospective multicenter assessment of survival in patients with IDH-mutant low-grade glioma based on adjuvant treatment. J Neurosurg 2019:1–8 doi 10.3171/2019.4.JNS183395.
5. Miller JJ, Gonzalez Castro LN, McBrayer S, Weller M, Cloughesy T, Portnow J, et al. Isocitrate dehydrogenase (IDH) mutant gliomas: A Society for Neuro-Oncology (SNO) consensus review on diagnosis, management, and future directions. Neuro Oncol 2023;25(1):4–25 doi 10.1093/neuonc/noac207. [PubMed: 36239925]
6. Buckner JC, Shaw EG, Pugh SL, Chakravarti A, Gilbert MR, Barger GR, et al. Radiation plus Procarbazine, CCNU, and Vincristine in Low-Grade Glioma. N Engl J Med 2016;374(14):1344–55 doi 10.1056/NEJMoa1500925. [PubMed: 27050206]
7. Feigenberg SJ, Amdur RJ, Morris CG, Mendenhall WM, Marcus RB, Jr., Friedman WA. Oligodendroglioma: does deferring treatment compromise outcome? Am J Clin Oncol 2003;26(3):e60–6 doi 10.1097/01.COC.0000072507.25834.D6. [PubMed: 12796617]
8. Wessels PH, Weber WE, Raven G, Ramaekers FC, Hopman AH, Twijnstra A. Supratentorial grade II astrocytoma: biological features and clinical course. Lancet Neurol 2003;2(7):395–403 doi 10.1016/s1474-4422(03)00434-4. [PubMed: 12849117]

9. van den Bent MJ, Wefel JS, Schiff D, Taphoorn MJ, Jaeckle K, Junck L, et al. Response assessment in neuro-oncology (a report of the RANO group): assessment of outcome in trials of diffuse low-grade gliomas. Lancet Oncol 2011;12(6):583–93 doi 10.1016/S1470-2045(11)70057-2. [PubMed: 21474379]
10. Ellingson BM, Bendszus M, Boxerman J, Barboriak D, Erickson BJ, Smits M, et al. Consensus recommendations for a standardized Brain Tumor Imaging Protocol in clinical trials. Neuro Oncol 2015;17(9):1188–98 doi 10.1093/neuonc/nov095. [PubMed: 26250565]
11. Wen PY, Chang SM, Van den Bent MJ, Vogelbaum MA, Macdonald DR, Lee EQ. Response Assessment in Neuro-Oncology Clinical Trials. J Clin Oncol 2017;35(21):2439–49 doi 10.1200/JCO.2017.72.7511. [PubMed: 28640707]
12. van den Bent MJ, Afra D, de Witte O, Ben Hassel M, Schraub S, Hoang-Xuan K, et al. Long-term efficacy of early versus delayed radiotherapy for low-grade astrocytoma and oligodendroglioma in adults: the EORTC 22845 randomised trial. Lancet 2005;366(9490):985–90 doi 10.1016/S0140-6736(05)67070-5. [PubMed: 16168780]
13. Mandonnet E, Delattre JY, Tanguy ML, Swanson KR, Carpentier AF, Duffau H, et al. Continuous growth of mean tumor diameter in a subset of grade II gliomas. Ann Neurol 2003;53(4):524–8 doi 10.1002/ana.10528. [PubMed: 12666121]
14. Rees J, Watt H, Jager HR, Benton C, Tozer D, Tofts P, et al. Volumes and growth rates of untreated adult low-grade gliomas indicate risk of early malignant transformation. Eur J Radiol 2009;72(1):54–64 doi 10.1016/j.ejrad.2008.06.013. [PubMed: 18632238]
15. Pallud J, Blonski M, Mandonnet E, Audureau E, Fontaine D, Sanai N, et al. Velocity of tumor spontaneous expansion predicts long-term outcomes for diffuse low-grade gliomas. Neuro Oncol 2013;15(5):595–606 doi 10.1093/neuonc/nos331. [PubMed: 23393207]
16. Pallud J, Mandonnet E, Duffau H, Kujas M, Guillevin R, Galanaud D, et al. Prognostic value of initial magnetic resonance imaging growth rates for World Health Organization grade II gliomas. Ann Neurol 2006;60(3):380–3 doi 10.1002/ana.20946. [PubMed: 16983683]
17. Brasil Caseiras G, Ciccarelli O, Altmann DR, Benton CE, Tozer DJ, Tofts PS, et al. Low-grade gliomas: six-month tumor growth predicts patient outcome better than admission tumor volume, relative cerebral blood volume, and apparent diffusion coefficient. Radiology 2009;253(2):505–12 doi 10.1148/radiol.2532081623. [PubMed: 19789244]
18. Huang RY, Young RJ, Ellingson BM, Veeraraghavan H, Wang W, Tixier F, et al. Volumetric analysis of IDH-mutant lower-grade glioma: a natural history study of tumor growth rates before and after treatment. Neuro Oncol 2020;22(12):1822–30 doi 10.1093/neuonc/noaa105. [PubMed: 32328652]
19. Ellingson BM, Kim GHJ, Brown M, Lee J, Salamon N, Steelman L, et al. Volumetric measurements are preferred in the evaluation of mutant IDH inhibition in non-enhancing diffuse gliomas: Evidence from a phase I trial of ivosidenib. Neuro Oncol 2022;24(5):770–8 doi 10.1093/neuonc/noab256. [PubMed: 34751786]
20. Mellinghoff IK, Ellingson BM, Touat M, Maher E, De La Fuente MI, Holdhoff M, et al. Ivosidenib in Isocitrate Dehydrogenase 1-Mutated Advanced Glioma. J Clin Oncol 2020;38(29):3398–406 doi 10.1200/JCO.19.03327. [PubMed: 32530764]
21. Mellinghoff IK, Penas-Prado M, Peters KB, Burris HA, 3rd, Maher EA, Janku F, et al. Vorasidenib, a Dual Inhibitor of Mutant IDH1/2, in Recurrent or Progressive Glioma; Results of a First-in-Human Phase I Trial. Clin Cancer Res 2021;27(16):4491–9 doi 10.1158/1078-0432.CCR-21-0611. [PubMed: 34078652]
22. Mellinghoff IK, Lu M, Wen PY, Taylor JW, Maher EA, Arrillaga-Romany I, et al. Vorasidenib and ivosidenib in IDH1-mutant low-grade glioma: a randomized, perioperative phase 1 trial. Nat Med 2023 doi 10.1038/s41591-022-02141-2.
23. Mellinghoff IK, van den Bent MJ, Blumenthal DT, Touat M, Peters KB, Clarke J, et al. Vorasidenib in IDH1- or IDH2-Mutant Low-Grade Glioma. N Engl J Med 2023;389(7):589–601 doi 10.1056/NEJMoa2304194. [PubMed: 37272516]
24. Ellingson BM, Gerstner ER, Lassman AB, Chung C, Colman H, Cole PE, et al. Hypothetical generalized framework for a new imaging endpoint of therapeutic activity in early phase clinical trials in brain tumors. Neuro Oncol 2022;24(8):1219–29 doi 10.1093/neuonc/noac086. [PubMed: 35380705]

25. Harris PA, Taylor R, Minor BL, Elliott V, Fernandez M, O'Neal L, et al. The REDCap consortium: Building an international community of software platform partners. J Biomed Inform 2019;95:103208 doi 10.1016/j.jbi.2019.103208. [PubMed: 31078660]
26. Harris PA, Taylor R, Thielke R, Payne J, Gonzalez N, Conde JG. Research electronic data capture (REDCap)--a metadata-driven methodology and workflow process for providing translational research informatics support. J Biomed Inform 2009;42(2):377–81 doi 10.1016/j.jbi.2008.08.010. [PubMed: 18929686]
27. Jain R, Johnson DR, Patel SH, Castillo M, Smits M, van den Bent MJ, et al. "Real world" use of a highly reliable imaging sign: "T2-FLAIR mismatch" for identification of IDH mutant astrocytomas. Neuro Oncol 2020;22(7):936–43 doi 10.1093/neuonc/noaa041. [PubMed: 32064507]
28. Broen MPG, Smits M, Wijnenga MMJ, Dubbink HJ, Anten M, Schijns O, et al. The T2-FLAIR mismatch sign as an imaging marker for non-enhancing IDH-mutant, 1p/19q-intact lower-grade glioma: a validation study. Neuro Oncol 2018;20(10):1393–9 doi 10.1093/neuonc/noy048. [PubMed: 29590424]
29. Patel SH, Poisson LM, Brat DJ, Zhou Y, Cooper L, Snuderl M, et al. T2-FLAIR Mismatch, an Imaging Biomarker for IDH and 1p/19q Status in Lower-grade Gliomas: A TCGA/TCIA Project. Clin Cancer Res 2017;23(20):6078–85 doi 10.1158/1078-0432.CCR-17-0560. [PubMed: 28751449]
30. Louis DN, Perry A, Reifenberger G, von Deimling A, Figarella-Branger D, Cavenee WK, et al. The 2016 World Health Organization Classification of Tumors of the Central Nervous System: a summary. Acta Neuropathol 2016;131(6):803–20 doi 10.1007/s00401-016-1545-1. [PubMed: 27157931]
31. Frampton GM, Fichtenholtz A, Otto GA, Wang K, Downing SR, He J, et al. Development and validation of a clinical cancer genomic profiling test based on massively parallel DNA sequencing. Nat Biotechnol 2013;31(11):1023–31 doi 10.1038/nbt.2696. [PubMed: 24142049]
32. Cheng DT, Mitchell TN, Zehir A, Shah RH, Benayed R, Syed A, et al. Memorial Sloan Kettering-Integrated Mutation Profiling of Actionable Cancer Targets (MSK-IMPACT): A Hybridization Capture-Based Next-Generation Sequencing Clinical Assay for Solid Tumor Molecular Oncology. J Mol Diagn 2015;17(3):251–64 doi 10.1016/j.jmoldx.2014.12.006. [PubMed: 25801821]
33. Louis DN, Perry A, Wesseling P, Brat DJ, Cree IA, Figarella-Branger D, et al. The 2021 WHO Classification of Tumors of the Central Nervous System: a summary. Neuro Oncol 2021;23(8):1231–51 doi 10.1093/neuonc/noab106. [PubMed: 34185076]
34. Cohen A, Sato M, Aldape K, Mason CC, Alfaro-Munoz K, Heathcock L, et al. DNA copy number analysis of Grade II-III and Grade IV gliomas reveals differences in molecular ontogeny including chromothripsis associated with IDH mutation status. Acta Neuropathol Commun 2015;3:34 doi 10.1186/s40478-015-0213-3. [PubMed: 26091668]
35. Aoki K, Nakamura H, Suzuki H, Matsuo K, Kataoka K, Shimamura T, et al. Prognostic relevance of genetic alterations in diffuse lower-grade gliomas. Neuro Oncol 2018;20(1):66–77 doi 10.1093/neuonc/nox132. [PubMed: 29016839]
36. Appay R, Dehais C, Maurage CA, Alentorn A, Carpentier C, Colin C, et al. CDKN2A homozygous deletion is a strong adverse prognosis factor in diffuse malignant IDH-mutant gliomas. Neuro Oncol 2019;21(12):1519–28 doi 10.1093/neuonc/noz124. [PubMed: 31832685]
37. Shirahata M, Ono T, Stichel D, Schrimpf D, Reuss DE, Sahm F, et al. Novel, improved grading system(s) for IDH-mutant astrocytic gliomas. Acta Neuropathol 2018;136(1):153–66 doi 10.1007/s00401-018-1849-4. [PubMed: 29687258]
38. Brat DJ, Aldape K, Colman H, Figrarella-Branger D, Fuller GN, Giannini C, et al. cIMPACT-NOW update 5: recommended grading criteria and terminologies for IDH-mutant astrocytomas. Acta Neuropathol 2020;139(3):603–8 doi 10.1007/s00401-020-02127-9. [PubMed: 31996992]
39. Mirchia K, Sathe AA, Walker JM, Fudym Y, Galbraith K, Viapiano MS, et al. Total copy number variation as a prognostic factor in adult astrocytoma subtypes. Acta Neuropathol Commun 2019;7(1):92 doi 10.1186/s40478-019-0746-y. [PubMed: 31177992]
40. Karschnia P, Vogelbaum MA, van den Bent M, Cahill DP, Bello L, Narita Y, et al. Evidence-based recommendations on categories for extent of resection in diffuse glioma. Eur J Cancer 2021;149:23–33 doi 10.1016/j.ejca.2021.03.002. [PubMed: 33819718]

41. Ellingson BM, Gerstner ER, Lassman AB, Chung C, Colman H, Cole PE, et al. Hypothetical Generalized Framework for a New Imaging Endpoint of Therapeutic Activity in Early Phase Clinical Trials in Brain Tumors. Neuro Oncol 2022 doi 10.1093/neuonc/noac086.

42. Pallud J, Varlet P, Devaux B, Geha S, Badoual M, Deroulers C, et al. Diffuse low-grade oligodendrogliomas extend beyond MRI-defined abnormalities. Neurology 2010;74(21):1724–31 doi 10.1212/WNL.0b013e3181e04264. [PubMed: 20498440]

43. Pallud J, Llitjos JF, Dhermain F, Varlet P, Dezamis E, Devaux B, et al. Dynamic imaging response following radiation therapy predicts long-term outcomes for diffuse low-grade gliomas. Neuro Oncol 2012;14(4):496–505 doi 10.1093/neuonc/nos069. [PubMed: 22416109]

44. Pallud J, Taillandier L, Capelle L, Fontaine D, Peyre M, Ducray F, et al. Quantitative morphological magnetic resonance imaging follow-up of low-grade glioma: a plea for systematic measurement of growth rates. Neurosurgery 2012;71(3):729–39; discussion 39-40 doi 10.1227/NEU.0b013e31826213de. [PubMed: 22668885]

45. Kickingereder P, Isensee F, Tursunova I, Petersen J, Neuberger U, Bonekamp D, et al. Automated quantitative tumour response assessment of MRI in neuro-oncology with artificial neural networks: a multicentre, retrospective study. Lancet Oncol 2019;20(5):728–40 doi 10.1016/S1470-2045(19)30098-1. [PubMed: 30952559]

46. Chang K, Beers AL, Bai HX, Brown JM, Ly KI, Li X, et al. Automatic assessment of glioma burden: a deep learning algorithm for fully automated volumetric and bidimensional measurement. Neuro Oncol 2019;21(11):1412–22 doi 10.1093/neuonc/noz106. [PubMed: 31190077]

47. Reis GF, Pekmezci M, Hansen HM, Rice T, Marshall RE, Molinaro AM, et al. CDKN2A loss is associated with shortened overall survival in lower-grade (World Health Organization Grades II-III) astrocytomas. J Neuropathol Exp Neurol 2015;74(5):442–52 doi 10.1097/NEN.0000000000000188. [PubMed: 25853694]

48. Marker DF, Pearce TM. Homozygous deletion of CDKN2A by fluorescence in situ hybridization is prognostic in grade 4, but not grade 2 or 3, IDH-mutant astrocytomas. Acta Neuropathol Commun 2020;8(1):169 doi 10.1186/s40478-020-01044-y. [PubMed: 33081848]

49. Tesileanu CMS, van den Bent MJ, Sanson M, Wick W, Brandes AA, Clement PM, et al. Prognostic significance of genome-wide DNA methylation profiles within the randomized, phase 3, EORTC CATNON trial on non-1p/19q deleted anaplastic glioma. Neuro Oncol 2021;23(9):1547–59 doi 10.1093/neuonc/noab088. [PubMed: 33914057]

50. Brand F, Forster A, Christians A, Bucher M, Thome CM, Raab MS, et al. FOCAD loss impacts microtubule assembly, G2/M progression and patient survival in astrocytic gliomas. Acta Neuropathol 2020;139(1):175–92 doi 10.1007/s00401-019-02067-z. [PubMed: 31473790]

Translational Relevance

Gliomas that carry mutations in isocitrate-dehydrogenase genes (IDH-mt) comprise a group of primary brain tumors with distinct clinical and radiographic behavior, governed by prognostically powerful molecular markers. Since IDH-mt gliomas demonstrate slow growth with relatively long survival periods, there is an urgent need for intermediate endpoints of disease progression. We hypothesized that tumor volumetric growth rates (TVGR) during observation correlate with key molecular signatures as well as next intervention-free and overall survival. Using log-linear mixed modeling, IDH-mt gliomas under observation after resection grew continuously with a %TVGR per 6 months around ~10% with a doubling time of 3.5 years. TVGR were significantly faster in gliomas harboring higher molecular grading such as homozygous deletion of CDKN2A/B. Longitudinal course of TVGR correlated with next intervention-free and overall survival. As novel IDH-targeted therapies enter clinical trials, development of surrogate endpoints through integration of radiological and molecular features of glioma will accelerate drug discovery.

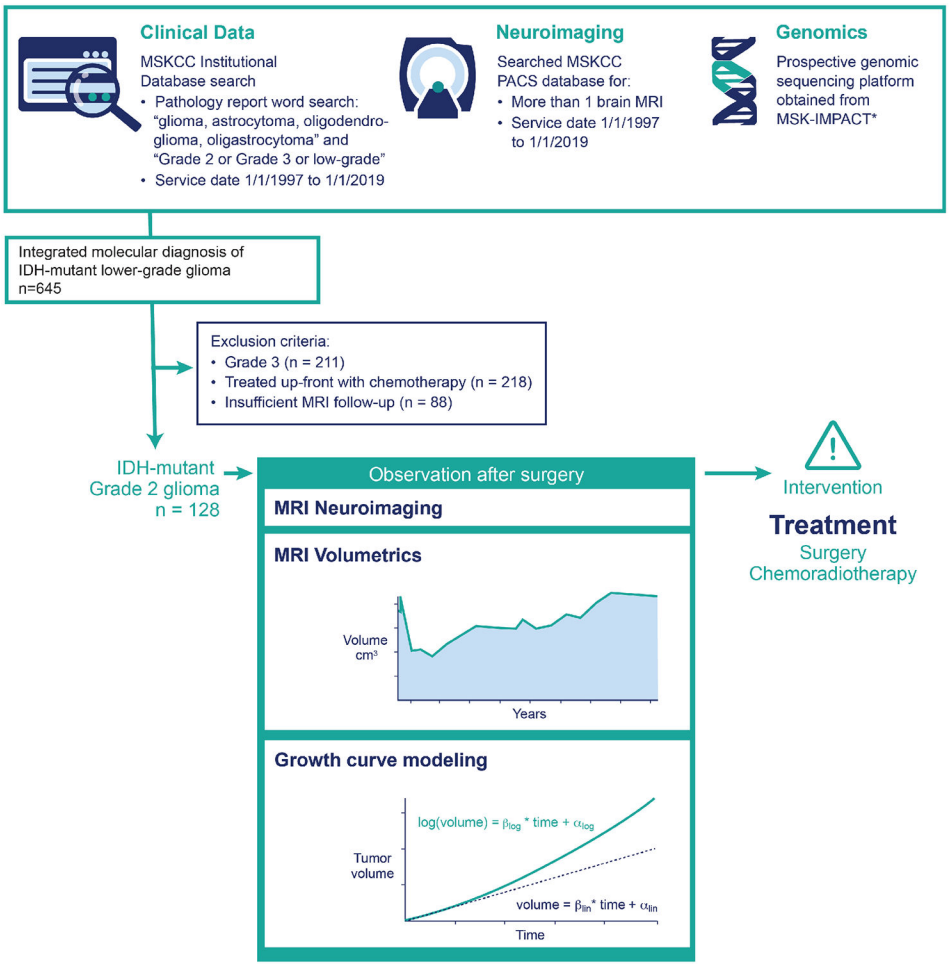

Figure 1. CONSORT diagram and schematic overview for this study.

Clinical data, neuroimaging, and genomic data were acquired using MSKCC's Institutional Database leading to an integrated molecular diagnosis. IDH-mt gliomas were subsequently analyzed in a multi-dimensional approach involving neuroimaging, volumetrics, and growth curve modeling.

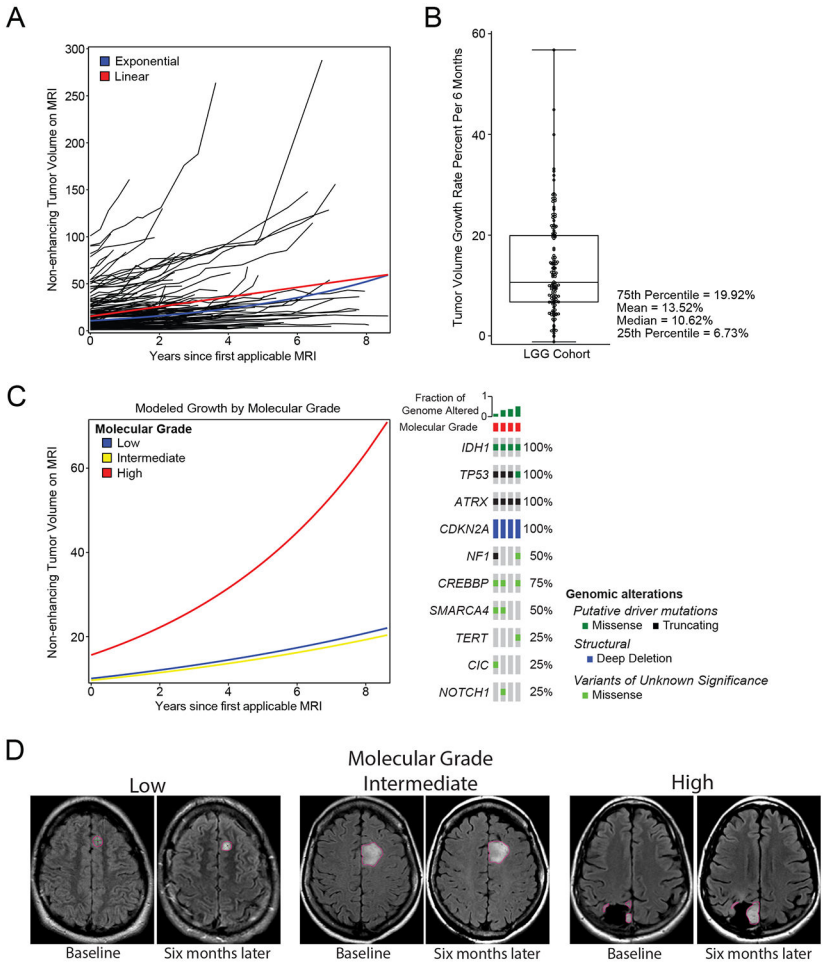

Figure 2. Tumor Volume Growth Rates and Molecular Grading.

A) Individual patient growth trajectories in the entire cohort for IDH-mutant low-grade gliomas with representative linear (red) and exponential (blue) growth models. **B)** The distribution of tumor volume growth rates per 6 months in the IDH-mutant glioma cohort. **C)** Low, intermediate, and high molecular grade IDH-mt gliomas are plotted with associated exponential model-based trajectories. **D)** Representative neuroimaging of an individual patient with low, intermediate, and high molecular grade growth.

Table 1.

Cohort characteristics, initial post-operative period of active surveillance (N=128).

Clinical Characteristic	Category	All Patients		1p19q co-deleted		1p19q intact		P
		N	%	N	%	N	%	
Patients (N)		128	100	69	53.9	59	46.1	--
Sex	Female	61	47.7	32	46.4	29	49.2	0.75
	Male	67	52.3	37	53.6	30	50.9	
Age at diagnostic surgery (first post-operative period)	Median (IQR)	37.8	31.6-46.3	41.3	35.2-50.4	32.8	26.2-39.3	**<0.001**
	< 40	77	60.2	32	46.4	45	76.3	**<0.001**
	40-60	43	33.6	33	47.8	10	17.0	
	> 60	8	6.3	4	5.8	4	6.8	
Presenting neurological symptom	Seizure	80	62.5	44	63.8	36	61.0	0.75
	Headache	19	14.8	11	15.9	8	13.6	0.71
	Cognition	11	8.6	8	11.6	3	5.1	0.19
	Numbness or tingling	8	6.3	5	7.3	3	5.1	0.72
	Dizziness	8	6.3	4	5.8	4	6.8	1.00
	Word finding difficulty	7	5.5	4	5.8	3	5.1	1.00
	Other[a]	16	12.5	7	10.1	9	15.3	0.38
	Asymptomatic (none of the above)	6	4.7	2	2.9	4	6.8	0.41
IDH genotype	IDH R132H positive by immunohistochemistry	120	93.8	64	92.8	56	94.9	0.61
	Next-generation sequencing	73	57	44	63.8	29	49.2	**0.01**
Number of MRI scans available for analyses	Postoperative after diagnostic surgery: Median (Range)	8	2-28	9	2-28	7	2-20	0.13
Follow-up	Years from first postoperative period after diagnostic surgery: Median (Range)	6.3	0.5-23.1	6.1	1.0-21.2	6.5	0.5-23.1	0.91

Abbreviations: N: Number; P: P-value; IQR: Interquartile Range; IDH: Isocitrate Dehydrogenase; MRI: Magnetic Resonance Imaging.

[a]Other comprises vision, weakness, fatigue, nausea/constipation, sleep, vertigo, and/or ENT.

Table 2.

Tumor Volume Growth Rates with Tumor Size and Extent of Resection.

			Log Linear Mixed Model (Percent Tumor Volume Growth Rate per 6 months, weighted by follow-up time per patient)		
Group	**1p19q Status**	**N**	**Modeled Growth**	**95% CI**	**P-value**
Overall Cohort	Intact and Codeleted	128	10.46%	9.11%, 11.83%	--
	Intact	59	11.73%	9.11%, 14.41%	0.16
	Codeleted	69	9.62%	8.26%, 10.99%	
Initial tumor size (postoperative): <25cm^3	Intact and Codeleted	95	10.55%	8.94%, 12.19%	0.68
Initial tumor size (postoperative): ≥25cm^3	Intact and Codeleted	33	10.06%	8.37%, 11.78%	
Near Total[a] Resection	Codeleted	14	10.98%	7.44%, 14.64%	0.20
Subtotal[b] Resection	Codeleted	35	9.17%	7.45%, 10.90%	
Partial[c] Resection	Codeleted	20	8.83%	7.08%, 10.61%	
Near Total[a] Resection	Intact	18	9.24%	5.08%, 13.58%	
Subtotal[b] Resection	Intact	28	13.47%	9.42%, 17.69%	
Partial[c] Resection	Intact	13	12.74%	8.71%, 16.92%	

Abbreviations: N: Number; CI: Confidence Interval; cm: Centimeter.

[a]Near total resection of T2/FLAIR-hyperintense tumore ≤5cm^3 residual T2/FLAIR-hyperintense tumor.

[b]Subtotal resection<25cm^3 residual T2/FLAIR-hyperintense residual tumor.

[c]Partial resection ≥25cm^3 residual tumor.

Table 3.

Doubling time during active surveillance.

Group	N	Doubling Time in Yearly Periods	95% CI
Overall Cohort	128	3.5	3.10-3.98
1p19q Intact	59	3.1	2.57-3.98
1p19q Codeleted	69	3.8	3.32-4.37
Low Molecular Grade	48	3.8	3.11-4.91
Intermediate Molecular Grade	21	4.0	3.19-5.30
High Molecular Grade	4	2.0	1.68-2.40

Abbreviations: N: Number; CI: Confidence Interval.

Table 4.

Tumor Volume Growth Rates and Molecular Grade.

		Log Linear Mixed Model (Percent Tumor Volume Growth Rate per 6 months, weighted by follow-up time per patient)		
Group	**N**	**Modeled Growth**	**95% CI**	**P-value**
Low Molecular Grade	48	9.54%	7.32%, 11.80%	<0.0001
Intermediate Molecular Grade	21	9.09%	6.76%, 11.46%	
High Molecular Grade	4	19.17%	15.57%, 22.89%	

Abbreviations: N: Number; CI: Confidence Interval.